

Published in final edited form as:

*Gene Ther.* 2006 January ; 13(1): 8–19. doi:10.1038/sj.gt.3302589.

## Adenoviral gene transfer of Akt enhances myocardial contractility and intracellular calcium handling

A Cittadini<sup>1</sup>, MG Monti<sup>1</sup>, G Iaccarino<sup>1</sup>, F Di Rella<sup>1</sup>, PN Tschlis<sup>2</sup>, A Di Gianni<sup>1</sup>, H Strömer<sup>3</sup>, D Sorriento<sup>1</sup>, C Peschle<sup>4</sup>, B Trimarco<sup>1</sup>, L Saccà<sup>1</sup>, and G Condorelli<sup>5,6</sup>

<sup>1</sup>Department of Clinical Medicine and Cardiovascular Sciences, University 'Federico II', Naples, Italy

<sup>2</sup>Molecular Oncology Research Institute, Tufts, New England Medical Center, Boston, MA, USA

<sup>3</sup>Medizinische Universitätsklinik, Würzburg, Germany

<sup>4</sup>Instituto Superiore Sanita', Rome, Italy

<sup>5</sup>San Raffaele Biomedical Science Park, Rome-Multimedica Hospital, Milan, Italy

<sup>6</sup>Institute of Molecular Medicine, University of California, San Diego, CA, USA

### Abstract

The serine-threonine kinase Akt/PKB mediates stimuli from different classes of cardiomyocyte receptors, including the growth hormone/insulin like growth factor and the  $\beta$ -adrenergic receptors. Whereas the growth-promoting and antiapoptotic properties of Akt activation are well established, little is known about the effects of Akt on myocardial contractility, intracellular calcium ( $\text{Ca}^{2+}$ ) handling, oxygen consumption, and  $\beta$ -adrenergic pathway. To this aim, Sprague–Dawley rats were subjected to a wild-type Akt in vivo adenoviral gene transfer using a catheter-based technique combined with aortopulmonary crossclamping. Left ventricular (LV) contractility and intracellular  $\text{Ca}^{2+}$  handling were evaluated in an isolated isovolumic buffer-perfused, aequorin-loaded whole heart preparations 10 days after the surgery. The  $\text{Ca}^{2+}$ –force relationship was obtained under steady-state conditions in tetanized muscles. No significant hypertrophy was detected in adenovirus with wild-type Akt (Ad.Akt) versus controls rats (LV-to-body weight ratio  $2.6 \pm 0.2$  versus  $2.7 \pm 0.1$  mg/g, controls versus Ad.Akt, P, NS). LV contractility, measured as developed pressure, increased by 41% in Ad.Akt. This was accounted for by both more systolic  $\text{Ca}^{2+}$  available to the contractile machinery (+19% versus controls) and by enhanced myofilament  $\text{Ca}^{2+}$  responsiveness, documented by an increased maximal  $\text{Ca}^{2+}$ -activated pressure (+19% versus controls) and a shift to the left of the  $\text{Ca}^{2+}$ –force relationship. Such increased contractility was paralleled by a slight increase of myocardial oxygen consumption (14%), while titrated dose of dobutamine providing similar inotropic effect augmented oxygen consumption by 39% ( $P < 0.01$ ). Phospholamban, calsequestrin, and ryanodine receptor LV mRNA and protein content were not different among the study groups, while sarcoplasmic reticulum  $\text{Ca}^{2+}$  ATPase protein levels were significantly increased in Ad.Akt rats.  $\beta$ -Adrenergic receptor density, affinity, kinase-1 levels, and adenylyl cyclase activity were similar in the three animal groups. In conclusion, our results support an important role for Akt/PKB in the regulation of myocardial contractility and mechanoenergetics.

© 2005 Nature Publishing Group All rights reserved

Correspondence: Dr A Cittadini, Department of Internal Medicine and Cardiovascular Sciences, University 'Federico II', Via S Pansini, 5 ed 18, Naples 80131, Italy. cittadin@unina.it.

Presented in part at the Annual La Jolla-Kyoto-Horizons on heart failure, La Jolla, CA, December 16–19, 2002.

## Keywords

Akt; heart; calcium; oxygen consumption

---

## Introduction

Akt (or protein kinase B) is a serine threonine kinase, which mediates signals from different classes of receptors. Particularly, it is activated by receptors endowed with intrinsic tyrosin kinase (e.g. insulin growth factor (IGF)-1 or insulin receptor), seven-membrane G-protein-coupled receptors (e.g.  $\beta$ -adrenergic receptor), gp130-dependent cytokines (e.g. interleukin-6), and estrogens.<sup>1–4</sup> Akt phosphorylation occurs primarily through phosphoinositide 3-kinase (PI3K) activation, translocating the kinase to the membrane.<sup>4</sup> The relevant downstream effectors of Akt are less clear, but include glycogen synthase kinase 3 (GSK-3), tuberous sclerosis complex 1–2, and members of the apoptotic cascade. The principal and most extensively investigated physiological actions of Akt consist of growth activation and apoptosis inhibition, both consistently documented in many systems.<sup>4–9</sup> However, it appears that Akt may also be involved in the regulation of myocardial contractility. A recently generated transgenic mouse with cardiac-restricted overexpression of constitutively active Akt, the E40K, exhibited a phenotype characterized not only by cardiomyocyte hypertrophy but also by a remarkable increase of myocardial contractility.<sup>10</sup> In this model of enhanced Akt activity, there is a marked upregulation of myocardial sarcoplasmic reticulum  $\text{Ca}^{2+}$  ATPase (SERCA-2) protein, and an increase of  $\text{Ca}^{2+}$  transients and channel currents.<sup>11</sup> However, the consequences of a transient elevation of Akt myocardial signaling on contractility and  $\text{Ca}^{2+}$  handling, particularly on  $\text{Ca}^{2+}$  responsiveness of the myofilaments in the normal myocardium, independent of the confounding effects of cardiac growth *in vivo*, are unknown. Equally unexplored are the mechanoenergetics responses to Akt overexpression that appear particularly relevant in view of the proposed therapeutic use of Akt in ischemia–reperfusion injury and heart failure.

Therefore, to address these issues, adenoviral gene transfer with Akt was performed in rats using a catheter-based technique coupled with aortopulmonary cross-clamping and coronary retroperfusion. At 10 days after gene transfer, hearts were harvested, aequorin-loaded and buffer-perfused in an isolated isovolumic Langendorff apparatus. Specifically, experiments were designed to address the following questions:

1. To ascertain the changes in  $\text{Ca}^{2+}$  handling potentially responsible for the positive inotropic actions of Akt by measuring intracellular-free  $\text{Ca}^{2+}$  concentrations,  $[\text{Ca}^{2+}]_i$ , using the photoprotein aequorin and by evaluating the maximal response and the sensitivity of the myofilaments to  $\text{Ca}^{2+}$  by plotting various  $[\text{Ca}^{2+}]_i$  and the corresponding force under steady-state conditions in tetanized muscles.
2. To explore the mechanoenergetics responses to elevated myocardial Akt signaling by comparing myocardial  $\text{O}_2$  consumption ( $\text{MVO}_2$ ) in Akt-transfected hearts and in hearts perfused with titrated doses of dobutamine.
3. To assess whether changes of the principal  $\text{Ca}^{2+}$ -regulating proteins including SERCA-2, phospholamban, calsequestrin, and ryanodine receptor or of the  $\beta$ -adrenergic signaling pathway are involved in Akt-induced increase of contractility.

Notably, experiments were performed only 10 days after gene transfer, to avoid the occurrence of significant cardiac growth *in vivo*.

## Results

### Cardiac gene transfer

We and others have previously demonstrated that the catheter-based aortopulmonary crossclamping with retrograde coronary perfusion yields stable, uniform, and efficient cardiac infection.<sup>12-14</sup> Immunohistochemistry analysis of cross-sectional myocardial slices sampled each millimeter with anti-hemoagglutinin (HA) monoclonal antibody showed that approximately 70% of cardiomyocytes were positive (Figure 1, panels a and b). Moreover, tissue histology analysis demonstrated a uniform distribution of the adenoviral infection with adenovirus with wild-type Akt (Ad.Akt) throughout the myocardium. No differences were noticed between the apical and the remaining area, where the aequorin macroinjection was performed. Control sections obtained by omitting the primary antibody showed no immuno-reaction (Figure 1, panels c and d). In the Ad.GFP-injected hearts, cardiomyocytes showed a similar percentage of infection and signal distribution compared with Ad.Akt group (Figure 1, panel g), but viral expression is also evident in the liver and kidney (Figure 1, panels h and i).

We then explored whether the adenoviral-mediated gene transfer of Akt resulted in increased protein expression and activation. Indeed, in the left ventricles exposed to the virus, we observed an increase in both the total amount and the phosphorylated Akt and phosphorylated GSK-3 (Figure 2). Accordingly, Akt activity assessed *in vitro* by GSK-3-GST fusion protein phosphorylation was significantly higher in the left ventricles exposed to the gene transfer (Figure 2).

Infected cardiac tissue displayed a slight inflammatory response with no evidence of tissue disruption nor increase of collagen deposition as assessed by picrosirius red staining. On the whole, left ventricular (LV) architecture appeared similar among the three study groups (Figure 1, panels e and f).

### Histology and echocardiography

Rats with myocardial Akt overexpression displayed no signs of cardiac growth, as documented by similar histological cardiomyocyte diameter among the study groups ( $17.42 \pm 3$  versus  $16.05 \pm 2.3$   $\mu\text{m}$  Ad.HA,  $17 \pm 4$   $\mu\text{m}$  Ad.GFP and  $16.58 \pm 2.5$   $\mu\text{m}$  controls). Lack of myocardial hypertrophy was further confirmed by echocardiography. Specifically, LV-to-body weight (BW) ratio was  $2.7 \pm 0.2$ ,  $2.6 \pm 0.3$ ,  $2.6 \pm 0.5$ , and  $2.7 \pm 0.3$  mg/g, in Ad.Akt, adenovirus tagged with the HA epitope (Ad.HA), Ad.GFP, and controls, respectively. LV systolic function, as assessed by endocardial fractional shortening, was increased by 20% in Ad.Akt rats compared with Ad.HA, Ad.GFP, and control saline-treated animals ( $45 \pm 3$  versus  $38 \pm 2$ ,  $38 \pm 4$ , and  $39 \pm 3\%$ , respectively,  $P < 0.05$ ).

### Effects of Akt on cardiac function and on $[\text{Ca}^{2+}]_i$ transients

Myocardial infection with Ad.HA and with Ad.GFP had no effects on cardiac function, as shown by the mechanical twitches similar to those of control rats (Table 1). On the contrary, Ad.Akt hearts displayed a significant increase of contractility. As a prototype, developed pressure was 41% higher than in controls rats, solely due to an increase in systolic pressure. Despite a longer mechanical twitch, diastolic function was not significantly altered by Ad.Akt, as shown by similar tau values in the four groups, which accurately measures LV relaxation, and by higher peak negative  $dP/dt$  (Table 1). The subcellular mechanisms of the inotropic effects of Ad.Akt were investigated in aequorin-loaded whole heart preparations in which  $[\text{Ca}^{2+}]_i$  transients and the corresponding pressure tracings were simultaneously recorded. Figure 3 shows a typical  $[\text{Ca}^{2+}]_i$  transient and the corresponding LV pressure tracing at baseline perfusate  $\text{Ca}^{2+}$  in the three study groups. The first relevant finding was

the association of increased developed pressure with a larger amplitude of the  $[Ca^{2+}]_i$  transient, which averaged 19%, in the absence of changes of diastolic  $[Ca^{2+}]_i$ . The time course of the transient was slightly but not significantly prolonged after Ad.Akt. Tau of the  $[Ca^{2+}]_i$  transient, which has been shown to reflect mostly the uptake of calcium by the sarcoplasmic reticulum,<sup>15</sup> was not significantly changed in Ad.Akt hearts, supporting the stance that the relaxation phase is not impaired by elevated myocardial Akt signaling. Since the magnitude of contractility change upon Akt adenoviral infection could not be explained only by increased  $Ca^{2+}$  available to the myofilament, a change in myofilament  $Ca^{2+}$  responsiveness was suggested. Indeed, maximal  $Ca^{2+}$ -activated pressure under tetanic conditions was significantly increased by 19%; the  $Ca^{2+}$ -concentration–response relationship was slightly shifted to the left, with  $EC_{50}$  values decreased by approximately 10% (Table 2). Figure 4 shows a representative tracing of intracellular  $Ca^{2+}$  and of corresponding pressure recorded under steady-state tetanic conditions in control and Ad.Akt-perfused hearts.

### Myocardial oxygen consumption

Myocardial oxygen consumption was evaluated as  $MVO_2$ . Dobutamine doses titrated to achieve a similar positive inotropic effect in isolated hearts caused an increase in  $MVO_2$  in Ad.Akt hearts, which was significantly smaller than that observed in control hearts (14 versus 39%, respectively,  $P < 0.01$ ) (Figure 5). This difference remained even after adjusting for heart rate (32 versus 12%,  $P < 0.01$ ).

### $N^G$ -nitro-L-arginine methyl ester (L-NAME)

To determine whether nitric oxide (NO) is involved in Akt-mediated positive inotropism, 12 additional rats were divided into the three study groups, and employed for additional perfusion studies. Specifically, four additional heart per each group were perfused with buffer plus the nonselective nitric oxide synthase (NOS) inhibitor, L-NAME (50  $\mu$ M). In the control and HA groups, the 50 L-NAME infusion induced a rapid  $8.2 \pm 2\%$  increase of coronary perfusion pressure, while LV developed pressure and  $+dP/dt$  remained unchanged ( $112 \pm 5$  versus  $112 \pm 4$  mmHg in control, and  $115 \pm 6$  versus  $115 \pm 4$  mmHg in Ad.HA, baseline and postinfusion values, respectively). In the Ad.Akt group, L-NAME application to the perfusate similarly increased coronary perfusion pressure by  $9 \pm 4\%$ , without affecting LV systolic and diastolic pressure. Thus, in this model system, NO does not appear to be involved in the increased contractility induced by Akt adenoviral gene transfer.

### Analysis of calcium-regulatory proteins

To gain further insight into the mechanisms of Akt-induced augmented contractility, we measured mRNA and protein LV content of four major calcium-regulating proteins including SERCA-2, which has been previously shown to be increased in Akt-overexpressing mice,<sup>11</sup> phospholamban, which is an important modulator of SERCA-2 activity, calsequestrin, an important SR  $Ca^{2+}$  buffer, and ryanodine receptor. Western blotting analysis revealed that LV protein levels of SERCA-2 (Figure 6) were significantly increased in Ad.Akt hearts compared with controls and Ad.HA ( $155 \pm 11$  and  $104 \pm 9\%$  of control values in Ad.Akt and Ad.HA groups, respectively,  $P < 0.01$ ), while phospholamban, ryanodine receptor, and calsequestrin levels were similar among the study groups (Figure 6).

No significant differences were detected with regard to the expression of the calcium-regulatory proteins mRNAs, as showed by Northern blot analysis (Figure 7).

## **$\beta$ -Adrenergic function**

No differences were found among the study groups in  $\beta$ -adrenergic receptor density and affinity and  $\beta$ -adrenergic receptor kinase 1 protein content (Figure 8). Therefore, neither downregulation of  $\beta$ -adrenergic receptor density nor alterations at the level of receptor coupling were present in conditions of elevated myocardial Akt signaling.

## **Discussion**

The current study demonstrates that Akt adenoviral gene transfer in normal hearts increases contractility. Such Akt-induced inotropic effects are independent of cardiac hypertrophy, and are secondary to both an increment of  $\text{Ca}^{2+}$  activator available to the contractile apparatus and to an augmented myofilament responsiveness to  $\text{Ca}^{2+}$ . Moreover, when compared with a typical inotropic stimulus such as that induced by dobutamine, the oxygen cost of pressure development is remarkably lower in Akt-infected hearts, indicating improved mechanical efficiency. Finally, while  $\beta$ -adrenergic receptor activation status is not affected by Akt activation, SERCA-2 protein level is significantly increased by 155% of control values, which may in part account for the observed changes in contractility. Upregulation of SERCA-2 appears mediated post-transcriptionally and is not associated with changes of myocardial mRNA and protein content of phospholamban, ryanodine receptor, and calsequestrin.

### **Contractile, $\text{Ca}^{2+}$ handling, and mechanoenergetics following Akt adenoviral gene transfer**

We provide the first evidence that the inotropic effect secondary to Akt activation, previously described only in chronic models of Akt overexpression, is independent of myocardial hypertrophy. Moreover, such contractile changes occur without significant impairment of diastolic function, at variance with other  $\text{Ca}^{2+}$  sensitizers.<sup>16,17</sup> As to the subcellular mechanisms underlying such positive inotropic effects, the contractile state of the muscle can be altered by several mechanisms: 'upstream' mechanisms, (1) altering the amplitude or time course of the  $[\text{Ca}^{2+}]_i$  transient, (2) altering the affinity of troponin C for  $\text{Ca}^{2+}$ , or downstream mechanisms such as (3) altering the response of the myofilaments to a given level of occupancy of the calcium binding sites on troponin C.<sup>16,17</sup> Viewed from this perspective, the changes of the  $\text{Ca}^{2+}$  transients observed in our study include a combination of such mechanisms. In fact, the amplitude of the transients was significantly increased compared to baseline. On the other hand, the increase in maximal  $\text{Ca}^{2+}$ -activated force observed in Ad.Akt rats speaks in favor of downstream mechanisms, that is, changes of myofilament kinetics after  $\text{Ca}^{2+}$  binding to troponin C.

In this regard, recent studies addressing the possibility that Akt mediates physiological hypertrophy have reported that controlled interval training increases cardiomyocyte contractility through a combination of higher myofilament  $\text{Ca}^{2+}$  sensitivity coupled with enhanced  $\text{Ca}^{2+}$  handling and increased SERCA-2 levels.<sup>18–19</sup>

Another distinct feature of Akt-positive inotropic action is that the increase in the amplitude of the mechanical twitch is accomplished without significant impairment of the myocardial relaxation, as shown by the similar tau values of the mechanical twitch in the four animal groups. This is further supported by the observation that intracellular  $\text{Ca}^{2+}$  decline is not different from controls, as shown by similar values of tau of the  $\text{Ca}^{2+}$  transients in Ad-Akt-infected hearts. On the other hand, tau of the  $\text{Ca}^{2+}$  transient has been proposed to depend primarily upon sarcoplasmic reticulum  $\text{Ca}^{2+}$  ATPase, the sarcolemma  $\text{Na}^+/\text{Ca}^{2+}$  exchanger, and buffering of  $\text{Ca}^{2+}$  by intracellular proteins, and its prolongation often precedes and causes abnormal myocardial relaxation.<sup>15</sup> These findings are at variance with other pure



myofilament  $\text{Ca}^{2+}$  sensitizers, whose action is almost invariably associated with variable degrees of myocardial relaxation impairment and slowed intra-cellular  $\text{Ca}^{2+}$  decline.<sup>16,17</sup>

A final interesting finding is the relatively low oxygen cost of pressure development induced by Akt activation. This may be explained by the  $\text{Ca}^{2+}$ -sensitizing effect, insofar as the reduction in the amounts of  $\text{Ca}^{2+}$  required to activate the myofilaments also lowers energy requirement for  $\text{Ca}^{2+}$  transport. Interestingly, also heart rate does not increase following elevated myocardial Akt signaling, which may further lower oxygen cost of pressure development compared with other inotropic agents inducing tachycardia. The use of sympathomimetic agents such as dobutamine or isoproterenol typically leads to a remarkable raise of  $\text{MVO}_2$  due to both heart rate and per beat  $\text{MVO}_2$  increase.<sup>20</sup> On the other hand, the decline of  $\text{MVO}_2$  upon administration of vasodilators such as nitroprusside or inhibitors of phosphodiesterase III that elevate cAMP and combine vasodilating and inotropic effects is not due to direct myocardial effect but is rather secondary to the vasodilation.<sup>21</sup>

### Comparison with previous studies

To date no study has addressed the mechanisms of enhanced cardiac function induced by elevated myocardial Akt signaling without the confounding impact of LV hypertrophy. Our data are congruent with the data obtained by Kim *et al.*<sup>11</sup> in conditions of remarkable myocardial hypertrophy (heart weight-to-body weight ratio in transgenic+60% versus wild-type animals), insofar as the magnitude of augmented myocyte contractile function (+74% transgenic versus wild-type animals) could not be solely explained by the 57% increase of Fura-2  $\text{Ca}^{2+}$  transients, but pointed to an increase of  $\text{Ca}^{2+}$  responsiveness of the myofilaments as a potential underlying mechanism. However, steady-state calcium concentration response were not obtained by Kim *et al.* Consistent is also the observation that Akt increases contractility without impairing myocardial relaxation. The differences concerning the magnitude of contractility increase, the level of SERCA-2 upregulation, can be explained by more prolonged myocardial exposure to higher levels of Akt overexpression, by the concomitant presence of cardiac hypertrophy, and by the different type of the Akt transgene, which in that study is a constitutively active form of Akt-1, while here we used the wild-type one. The IGF signaling pathway activates Akt through PI3K.<sup>4</sup> The growth-promoting and anti-apoptotic properties of IGF-1 activation are indeed partly mediated by Akt activation.<sup>4,6</sup> It has been proposed that myocardial Akt activation may also be involved in the structural and functional changes observed after long-term exposure to GH excess, as typically occurs in the acromegaly.<sup>5,22</sup> In the same model system, we have previously shown an increase of contractility averaging 20% following acute application of graded concentration of IGF-1 in the perfusate, mostly due to augmented  $\text{Ca}^{2+}$  responsiveness of the myofilaments.<sup>23</sup> Although it is difficult to compare the acute application of IGF-1 on isolated muscle preparations with increased Akt signaling due to *in vivo* gene transfer, it is possible that part of the IGF-1 effects on contractility may be mediated by Akt, although there are differences in the magnitude of contractility increase.

It therefore appears that Akt acts through different pathways known to affect myocardial mechanics, which is perfectly congruent with its critical position downstream of receptors with intrinsic tyrosin kinase activity (growth factors such as IGF-1 or insulin), IL6 family receptors, and seven-transmembrane G-protein-coupled receptors ( $\beta$ -receptors).<sup>1-4</sup> Moreover, the recent demonstration of a direct SERCA-2 upregulation in Akt-overexpressing mice<sup>11</sup> is in part supported by our data demonstrating a significant increase of SERCA-2 protein in Ad.Akt-infected rats. This finding, which was also observed in rats following exogenous GH administration,<sup>24</sup> provides potential molecular underpinnings for the contractility and  $\text{Ca}^{2+}$  handling changes observed in the current study. In fact, SERCA-2 overexpression is known to increase  $\text{Ca}^{2+}$  transport and cardiac function, and is mainly

characterized by increased systolic  $\text{Ca}^{2+}$  levels, shorter transients, enhanced contractility with accelerated rates of contraction and relaxation, and no evidence of diastolic  $\text{Ca}^{2+}$  overload consistent with the enhanced capacity of the SR to sequester calcium.<sup>25,26</sup> The mechanisms of SERCA-2 are likely complex, but do not involve significant changes of phospholamban, calsequestrin, and ryanodine receptor protein and transcripts levels, confirming previous data obtained in Akt-overexpressing mice.<sup>11</sup> However, the possibility of a change in the extent of phospholamban phosphorylation and its effect on SERCA-2 cannot be excluded. The increase of SERCA-2 in our model system is mediated by post-transcriptional mechanism, since SERCA-2 mRNA was not different among the three study groups. Further research is needed to clarify whether elevated myocardial Akt signaling is associated with enhanced translation or stability of SERCA-2.

### Clinical implications

Akt activation increases contractility with a combined mechanism of increase  $[\text{Ca}^{2+}]_i$ , and by sensitizing the myofilaments to  $\text{Ca}^{2+}$ , with marginal increase of myocardial oxygen consumption. The reduced oxygen consumption required for  $\text{Ca}^{2+}$  transport in turn limits the threat of arrhythmias, and may blunt  $\text{Ca}^{2+}$ -dependent transcriptional and translational mechanisms leading to hypertrophy and failure. Coupled with the well-established antiapoptotic and growth-promoting properties displayed by Akt in several model systems, the observed remarkable positive inotropic effects opens new scenarios regarding clinical heart disease. Indeed, changes in the activation status of Akt have been recently reported in experimental diabetic cardiomyopathy<sup>27</sup> and human heart failure,<sup>28</sup> thus painting Akt as a target for novel therapeutic strategies. To support this view, recent studies have demonstrated beneficial effects following elevated myocardial Akt signaling in experimental heart failure.<sup>29</sup>

### Materials and methods

#### Adenoviral constructs

We used replication-defective adenoviral vectors encoding for the human AKT1 wild-type gene included in a frame HA epitope 3'-tag (A.-AKT) under the control of the cytomegalovirus promoter, and as a control, a similar adenoviral vector encoding for the HA epitope.30:31 A small group of five animals (Ad.GFP) was injected with a similar adenoviral vector encoding for the reporter GFP fusion protein.

#### Experimental protocol

Sprague–Dawley male rats (Charles River, Italy, body weight (BW), 210–250 g) were randomized into three groups ( $n=11$  in each group +4 for L-NAME experiments and +5 injected with GFP, see below): saline treatment (sham), Ad.HA, and Ad.Akt.<sup>31</sup> The viral delivery procedure has been described previously in detail.<sup>12</sup> Briefly, rats were anesthetized with a mixture of ketamine hydrochloride (Sigma, 50 mg/kg BW) and xylazine (Sigma, 10 mg/kg BW) and then orally intubated and ventilated. The animals were subsequently cooled with ice bags and their temperature monitored with a thermistor catheter. A method based on that reported by Hajjar *et al.*<sup>13</sup> and subsequently modified by Ikeda *et al.*<sup>14</sup> was used to deliver the viral construct. When the animal's temperature reached 30°C, an anterior thoracotomy was performed, the heart was exteriorized, and a 7.0 suture placed on the apex of the left ventricle. A 22 G catheter containing 200  $\mu\text{l}$  of viral solution of  $1 \times 10^{12}$  PFU was then gently introduced into the left ventricle. The aortic root and pulmonary artery were identified and the catheter advanced through the left ventricle into the aortic root. The aorta and pulmonary artery were clamped gently, distal to the site of the catheter and the viral solution injected. The period of total occlusion (time for viral injection and the postinjection period) lasted 30 s, allowing the solution to circulate down the coronary arteries. Then, the

aortic and pulmonary clamps and the catheter were removed, the pneumothorax evacuated, and the chest closed. Animals were transferred back to their cages where they were allowed to recover. The same procedure was followed for sham-operated rats, but the catheter was filled with saline.

### Echocardiography

Transthoracic echocardiograms were performed in all surviving animals, according to previously described methods,<sup>32</sup> with a SONOS 5500 electronic system equipped with a 7 or 12 MHz probe (Agilent Technologies, MA, USA). All measurements, performed with an off-line analysis system by one observer who was blinded to prior results, were based on the average of three to six consecutive cardiac cycles.

### Perfusion technique

Rats were killed and the isolated hearts were placed in a isovolumic, buffer-perfused preparation according to the Langendorff technique, as described previously.<sup>23,33</sup> Briefly, the rats were anesthetized with ether, followed by an injection of 200 IU heparin in the femoral vein. After 1 min, the thorax was opened and the heart quickly removed and put into ice-cold Krebs–Henseleit solution (*vide infra*), weighed, and mounted on a cannula inserted into the ascending aorta. Retrograde aortic perfusion of the coronary arteries was performed within 30 s after the thoracotomy via a constant flow of 10 ml/min/g heart weight. Pressure was monitored by a Statham P23Db transducer. Cardiac temperature was set at 25°C, measured by a temperature probe inserted into the right ventricle. The composition of the perfusate was as follows (mM): NaCl 118, KCl 4.7, KH<sub>2</sub>PO<sub>4</sub> 1.2, CaCl<sub>2</sub> 2, MgCl<sub>2</sub> 1.2, NaHCO<sub>3</sub> 23, dextrose 5.5, and saturated with a 95% O<sub>2</sub>–5% CO<sub>2</sub> gas mixture to a pH of 7.4±0.2. LV pressure was measured using a fluid-filled latex balloon inserted into the left ventricle via the mitral valve. After an equilibration period of 15–30 min at 25°C, the temperature was gradually increased to 36°C and the hearts were paced at 3.5 Hz. Measurements of LV function were obtained when the preparation achieved a steady state after instrumentation (approximately 15 min); the balloon volume was inflated to achieve a diastolic pressure of 2–4 mmHg in all the animal groups.

The digital signal of the LV pressure tracing was further analyzed using customized software to obtain the following parameters: peak LV–systolic pressure, LV end–diastolic pressure, LV developed pressure, time to peak pressure, time from peak systolic pressure to 90% of relaxation, time constant of exponential pressure decay using the variable asymptote method, or tau, and maximum and minimum values of the first pressure derivative with respect to time. Every parameter was measured three times for each experimental point and was then averaged.

### Aequorin loading

Aequorin loading was performed as described previously.<sup>23,33</sup> Briefly, 3–5 µl of an aequorin containing solution (1 µg/ml) was macroinjected into the interstitium of the inferoapical region of the LV. The heart was then positioned in an organ bath with the aequorin-loaded area of the LV directed toward the cathode of a photomultiplier (model 9635QA, Thorn-EMI, Gencom Inc.) and submerged in Krebs–Henseleit solution. At 5–10 min after loading, which was performed under Ca<sup>2+</sup>-free conditions, CaCl<sub>2</sub> was gradually added to the coronary perfusate up to a total Ca<sup>2+</sup> concentration of 1 mmol/l. The experimental protocol was started 5–10 min after a steady state of the mechanical parameters was reached.



### Quantification of intracellular $\text{Ca}^{2+}$

Aequorin light signals were recorded on a four-channel recorder in parallel with the LV pressure and coronary perfusion pressure tracings and were digitized as described above for the LV pressure tracings. At each step of perfusate  $\text{Ca}^{2+}$ , 30–60 light transients were wave averaged, and values were converted into intracellular  $\text{Ca}^{2+}$  concentrations using the method of fractional luminescence as described previously.<sup>23,33</sup> At the end of each experiment, the heart was perfused with a solution containing 20 mmol/l  $\text{Ca}^{2+}$  and 5% Triton X-100 to lyse the aequorin-loaded cells and expose all of the remaining aequorin to  $\text{Ca}^{2+}$ . This resulted in an instantaneous burst of light, subsequently declining to baseline within 10–20 min. The area under the curve was integrated to obtain a value for  $L_{\text{max}}$ . The ratio of the light versus  $L_{\text{max}}$  is the fractional luminescence, which was converted into intracellular  $\text{Ca}^{2+}$  concentrations by the use of a calibration curve derived *in vitro*. The wave-averaged signals were analyzed for peak systolic  $\text{Ca}^{2+}$ , diastolic  $\text{Ca}^{2+}$ , time to peak light, time from peak light to 50% of light decay, and time constant of exponential light decay, tau, using the variable asymptote method.

### Analysis of the calcium concentration–response relationship

The response of the myofilament apparatus to  $\text{Ca}^{2+}$  consists of two terms: the myofilament  $\text{Ca}^{2+}$  sensitivity, which describes the affinity of the contractile apparatus for  $[\text{Ca}^{2+}]_i$  over the ranges of contractile responsiveness to  $[\text{Ca}^{2+}]_i$  (the  $\text{EC}_{50}$  of the  $\text{Ca}^{2+}$ -concentration–response relationship), and the maximal  $\text{Ca}^{2+}$  activated force, which determines the amplitude of the contractile response.<sup>16,17</sup> Both components were evaluated in the isolated whole heart by steady-state pressure– $\text{Ca}^{2+}$  relations obtained by eliciting tetanus with rapid pacing after exposure to ryanodine, according to a previously described technique.<sup>23,33</sup> Ryanodine  $10^{-7}$  M (Calbiochem, San Diego, CA, USA) was added to the perfusate to inhibit sarcoplasmic reticulum function. Typically, LV function declined gradually reaching a new steady state after about 20 min. Tetanus was then elicited by 4 s of high-frequency electrical stimulation (15 Hz) with a pulse width of 50 ms at 1.5–2.0 times the threshold. Tetanic pressures peaked after approximately 2 s, and tetanic light signals reached a plateau after 2–3 s. Tetanic responses at 0.5, 1.0, 2.0, 4.0, and 6.0 mM  $[\text{Ca}^{2+}]$  with repeated and averaged (3–5 tetani) measurements for peak tetanic pressure and light signals at each  $\text{Ca}^{2+}$  level were assessed. Sensitivity ( $\text{EC}_{50}$ ) and maximal  $\text{Ca}^{2+}$ -activated pressure of the calcium concentration–response relationship were obtained as described previously,<sup>23,33</sup> plotting peak tetanic pressure against peak systolic calcium.

### L-NAME

In another series of experiments, L-NAME 50  $\mu\text{M}$  was added to perfusate in control, Ad.HA, and Ad.Akt (four animals per each group) after the equilibration period, and all the above-mentioned parameters were monitored continuously, with 3–5 averaged measurements.

### Oxygen consumption

Coronary flow was determined by collecting coronary effluent for 60 s. Perfusate  $\text{PO}_2$  between the aortic perfusate with a blood gas analyzer (model ABL 510, Radiometer); arteriovenous oxygen difference was calculated from the difference in  $\text{PO}_2$  between the aortic perfusate and the coronary venous effluent, assuming a solubility of 0.023 ml  $\text{O}_2$  per milliliter of perfusate at 760 mmHg, and was expressed as micromoles per milliliter. Myocardial oxygen consumption was calculated as the product of arteriovenous oxygen difference and coronary flow and expressed as micromoles per minute per gram of left ventricle.<sup>34</sup> Each sample was assayed twice.

After recording baseline mechanical parameters, dobutamine was added to the perfusate in increasing steps starting from a concentration of  $10^{-8}$  M until reaching the same level of inotropic stimulation of Ad.Akt rats expressed as  $+dP/dt$ /developed pressure. Heart rate, inotropic, and lusitropic parameters of function (peak positive, peak negative  $dP/dt$  normalized to developed pressure, and time to 90% of relaxation) were recorded before and during continuous perfusion with dobutamine<sup>35</sup> with three averaged measurements for each step.

### Histology and immunohistochemistry

Formalin-fixed and paraffin-embedded myocardial sections were stained with hematoxylin-eosin (general morphology) or with picosirius red (collagen content) or were immunostained to evaluate adenoviral expression. The morphometric analyses were carried out on sections sampled each millimeter, from myocardial apex to base; a total of 40 fields each millimeter were evaluated.

Immunohistochemistry was performed with anti-HA antibody (Sigma, 1:50) followed by ABC (avidin-biotin complex) kit (Pierce) and diaminobenzidine (Pierce) chromogen as peroxidase substrate. Collagen content was expressed as the mean percentage of picosirius red-stained tissue areas divided by total tissue area in the same field; percentage of infected cardiomyocytes was expressed as the mean percentage of immunopositive myocytes with respect to total myocyte number in the same field. Two researchers blinded for the experimental protocols carried out all measurements independently.

### Akt, phosphorylated Akt, and total Akt activity

Left ventricles were homogenated in RIPA-SDS buffer (50 mM Tris-HCl (pH 7.5), 150 mM NaCl, 1% NP-40, 0.25% deoxycholate, 9.4 mg/50 ml sodium orthovanadate, 20% sodium dodecyl sulfate). Equal amount of protein from clarified homogenates were resolved by PAGE and transferred to nitrocellulose filter as described previously.<sup>30</sup> Total Akt, serine 473-phosphorylated Akt, phosphorylated GSK-3 and ERK2 were visualized by specific antibodies (Cell Signaling), followed by incubation with an anti-rabbit horseradish peroxidase (HRP)-conjugated secondary antibody (Santacruz Biotechnology) and standard chemiluminescence (Renaissance, NEN).

Akt kinase activity was analyzed as described previously.<sup>30</sup> LV extracts were incubated 2 h with immobilized Akt monoclonal antibody. After an extensive washing, the kinase reaction was performed at 30°C for 30 min in the presence of 200  $\mu$ M cold ATP and GSK-3 substrate. Phosphorylation of GSK-3 was measured by Western blot by using phospho-GSK-3 $\alpha/\beta$  (Ser-21/9) antibody. Autoradiographies were digitalized and quantified using Image Quant software (Molecular Dynamics) using ERK2 as loading control. Each sample was run in duplicate and two to three Western blotting were performed.

### Ca<sup>2+</sup>-regulatory proteins

For the analysis of calcium-regulatory proteins, cardiac tissue was quickly snap frozen in nitrogen and then homogenated as described in detail by Callies *et al.*<sup>36</sup> Proteins were separated with discontinuous PAGE with 4 and 17% acrylamide and transferred to polyvinylidene difluoride membranes; transfer efficiency was verified by Ponceau S staining of the protein bands. Membranes were incubated with antibodies against SERCA-2a (1:1500, Affinity Bioreagents), phospholamban (1:2000, Upstate Biotech.), and calsequestrin (1:2000, Upstate Biotech), which was detected for control. Immunoblots were then detected, enhanced, and evaluated as described above.

Three independent Western blots were performed for each antibody<sup>36</sup> and each sample was run in duplicate.

Cardiac RNA was extracted as described by Chomczynski *et al.*,<sup>37</sup> separated on 1.2% agarose-formaldehyde gel and Northern blotted as described previously.<sup>38</sup> Probes for SERCA-2, phospholamban, ryanodine receptor calsequestrin (from rabbit heart), and glyceralde-hyde-3 phosphate dehydrogenase (GAPDH) were 523, 2090, 535, 2400, and 428 bp, respectively.

Quantitative evaluation of each specific autoradio-gram was approached by normalizing the scanned densitometric intensity to the hybridization signal obtained with GAPDH from the same lane. The size of hybridized messengers was estimated using the 28S rRNA band as standard. Every probe was assayed in duplicate and two to three Northern Blotting were performed.

### **$\beta$ -Adrenoreceptor radioligand binding and kinase-1 immunoblotting**

Receptor binding on myocardial membranes was performed as previously described using the nonselective  $\beta$ AR ligand [<sup>125</sup>I]-cyanopindolol.<sup>39</sup> Competition binding isotherms in sarcolemmal membranes was performed as described previously<sup>39</sup> in triplicate with 12 varying concentration of isoproterenol ( $10^{-12}$ – $10^{-4}$  M). Assays were conducted at 37°C for 60 min and then filtered over glass fiber membranes (Skatron), washed, and counted in a  $\gamma$  counter. Competition curves were analyzed by nonlinear least-squares curve fit (Graph Pad Prism).

Immunodetection of left ventricle levels of  $\beta$ -adreno-receptor kinase-1 was performed on detergent-solubilized extracts by Western blot technique, using a polyclonal antibody (SC 562, Santacruz Biotechnology) and an HRP-conjugated goat anti-rabbit secondary antibody and visualized by chemiluminescence (Renaissance, NEN) on autoradiographic sheets. Blots were therefore digitalized and quantified by Image Quant software, as described previously.<sup>39</sup> Each assay was repeated twice and each sample was examined in duplicate.

### **Statistical analysis**

Data are reported as mean $\pm$ s.e.m. Between-group comparisons of echocardiographic indexes were performed using a two-way ANOVA with repeated measure in one factor (time), followed by Neumann–Keuls test. One-way ANOVA was employed for the other comparisons, also followed by Neumann–Keuls test. Percent differences of MVO<sub>2</sub> among the groups were compared using nonparametric tests. A *P*-value of <0.05 was considered significant.

### **Acknowledgments**

This work was supported in part by grants from the Italian National Institute of Health, The Italian Ministry of Education (MIUR), and Adriano Buzzati-Traverso Foundation.

### **References**

1. Testa JR, Bellacosa A. Akt plays a central role in tumorigenesis. *Proc Natl Acad Sci USA* 2001;98:10983–10985. [PubMed: 11572954]
2. Oh H, Fujio Y, Kunisada K, Hirota H, Matsui H, Kishimoto T, et al. Activation of phosphatidylinositol 3-kinase through glycoprotein 130 induces protein kinase B and p70 S6 kinase phosphorylation in cardiac myocytes. *J Biol Chem* 1998;273:9703–9710. [PubMed: 9545305]

3. Morisco C, Zebrowski DC, Vatner DE, Vatner SF, Sadoshima J. The Akt-glycogen synthase kinase 3beta pathway regulates transcription of atrial natriuretic factor induced by beta-adrenergic receptor stimulation in cardiac myocytes. *J Biol Chem* 2000;275:14466–14475. [PubMed: 10799529]
4. Matsui T, Nagoshi T, Rosenzweig A. Akt and PI 3-kinase signaling in cardiomyocyte hypertrophy and survival. *Cell Cycle* 2003;2:220–223. [PubMed: 12734428]
5. Shioi T, McMullen JR, Kang PM, Douglas PS, Obata T, Franke TF, et al. Akt/protein kinase B promotes organ growth in transgenic mice. *Mol Cell Biol* 2002;22:2799–2809. [PubMed: 11909972]
6. Yamashita K, Kajstura J, Discher DJ, Wasserlauf BJ, Bishopric NH, Anversa P, et al. Reperfusion-activated Akt kinase prevents apoptosis in transgenic mouse hearts overexpressing insulin-like growth factor-1. *Circ Res* 2001;88:609–614. [PubMed: 11282895]
7. Miao W, Luo Z, Kitsis RN, Walsh K. Intracoronary adenovirus-mediated Akt gene transfer in heart limits infarct size following ischemia–reperfusion injury *in vivo*. *J Mol Cell Cardiol* 2000;32:2397–2402. [PubMed: 11113015]
8. Matsui T, Tao J, del Monte F, Lee KH, Li L, Picard M, et al. Akt preserves cardiac function and prevents injury after transient cardiac ischemia *in vivo*. *Circulation* 2001;104:330–335. [PubMed: 11457753]
9. Fujio Y, Nguyen T, Wencker D, Kitsis RN, Walsh K. Akt promotes survival of cardiomyocytes *in vitro* and protects against ischemia–reperfusion injury in mouse heart. *Circulation* 2000;101:660–667. [PubMed: 10673259]
10. Condorelli G, Drusco A, Stassi G, Bellacosa A, Roncarati R, Iaccarino G, et al. Akt induces enhanced myocardial contractility and cell size *in vivo* in transgenic mice. *Proc Natl Acad Sci USA* 2002;99:12333–12338. [PubMed: 12237475]
11. Kim YK, Kim SJ, Yatani A, Huang Y, Castelli G, Vatner DE, et al. Mechanisms of enhanced cardiac function in mice with hypertrophy induced by overexpressed Akt. *J Biol Chem* 2003;278:47622–47628. [PubMed: 13129932]
12. Bonci D, Cittadini A, Latronico MV, Borello U, Aycock JK, Drusco A, et al. ‘Advanced’ generation lentiviruses as efficient vectors for cardiomyocyte gene transduction *in vitro* and *in vivo*. *Gene Therapy* 2003;10:630–636. [PubMed: 12692591]
13. Hajjar RJ, Schmidt U, Matsui T, Guerrero JL, Lee KH, Gwathmey JK, et al. Modulation of ventricular function through gene transfer *in vivo*. *Proc Natl Acad Sci USA* 1998;95:5251–5256. [PubMed: 9560262]
14. Ikeda Y, Gu Y, Iwanaga Y, Hoshijima M, Oh SS, Giordano FJ, et al. Restoration of deficient membrane proteins in the cardiomyopathic hamster by *in vivo* cardiac gene transfer. *Circulation* 2002;105:502–508. [PubMed: 11815435]
15. Camacho SA, Brandes R, Figueredo VM, Weiner MW. Ca<sup>2+</sup> transient decline and myocardial relaxation are slowed during low flow ischemia in rat hearts. *J Clin Invest* 1994;93:951–957. [PubMed: 8132781]
16. Blinks JR, Endoh M. Modification of myofibrillar responsiveness to Ca<sup>2+</sup> as an inotropic mechanism. *Circulation* 1986;73:III85–III98. [PubMed: 2867838]
17. Perrault CL, Meuse AJ, Bentivegna LA, Morgan JP. Abnormal intracellular calcium handling in acute and chronic heart failure: role in systolic and diastolic dysfunction. *Eur Heart J* 1990;11:8–21.
18. Wisloff U, Loennechen JP, Falck G, Beisvag V, Currie S, Smith G, et al. Increased contractility and calcium sensitivity in cardiac myocytes isolated from endurance trained rats. *Cardiovasc Res* 2001;50:495–508. [PubMed: 11376625]
19. Wisloff U, Loennechen JP, Currie S, Smith GL, Ellingsen O. Aerobic exercise reduces cardiomyocyte hypertrophy and increases contractility, Ca<sup>2+</sup> sensitivity and SERCA-2 in rat after myocardial infarction. *Cardiovasc Res* 2002;54:162–174. [PubMed: 12062372]
20. Beanlands RS, Bach DS, Raylman R, Armstrong WF, Wilson V, Montieth M, et al. Acute effects of dobutamine on myocardial oxygen consumption and cardiac efficiency measure using carbon-11 acetate kinetics in patients with dilated cardiomyopathy. *J Am Coll* 1993;22:1389–1398.

21. Hasenfuss G, Holubarsch C, Heiss HW, Meinertz T, Bonzel T, Wais U, et al. Myocardial energetics in patients with dilated cardiomyopathy: influence of nitroprusside and enoximone. *Circulation* 1989;80:51–64. [PubMed: 2525432]
22. Saccà L, Cittadini A, Fazio S. Growth hormone and the heart. *Endocr Rev* 1994;15:555–573. [PubMed: 7843068]
23. Cittadini A, Ishiguro Y, Stromer H, Spindler M, Moses AC, Clark R, et al. Insulin-like growth factor-1 but not growth hormone augments mammalian myocardial contractility by sensitizing the myofilament to  $\text{Ca}^{2+}$  through a wortmannin-sensitive pathway. Studies in rat and ferret isolated muscles. *Circ Res* 1998;83:50–59. [PubMed: 9670918]
24. Tajima M, Weinberg EO, Bartunek J, Jin H, Yang R, Paoni NF, et al. Treatment with growth hormone enhances contractile reserve and intracellular calcium transients in myocytes from rats with postinfarction heart failure. *Circulation* 1999;99:127–134. [PubMed: 9884389]
25. He H, Giordano FJ, Hilal-Dandan R, Choi DJ, Rockman HA, McDonough PM, et al. Overexpression of the rat sarcoplasmic reticulum  $\text{Ca}^{2+}$ -ATPase gene in the heart of transgenic mice accelerates calcium transients and cardiac relaxation. *J Clin Invest* 1997;100:380–389. [PubMed: 9218515]
26. Baker DL, Hashimoto K, Grupp IL, Ji Y, Reed T, Loukianov E, et al. Targeted overexpression of the sarcoplasmic reticulum  $\text{Ca}^{2+}$ -ATPase increases cardiac contractility in transgenic mouse hearts. *Circ Res* 1998;83:1205–1214. [PubMed: 9851937]
27. Duan J, Zhang HY, Adkins SD, Ren BH, Norby FL, Zhang X, et al. Impaired cardiac function and IGF-I response in myocyte from calmodulin-diabetic mice: role of Akt and RhoA. *Am J Physiol* 2003;284:E366–E376.
28. Haq S, Choukroun G, Lim H, Tymitz KM, del Monte F, Gwathmey J, et al. Differential activation of signal transduction pathways in human hearts with hypertrophy versus advanced heart failure. *Circulation* 2001;103:670–677. [PubMed: 11156878]
29. Taniyama Y, Walsh K. Elevated myocardial Akt signaling ameliorates doxorubicin-induced congestive heart failure and promotes heart growth. *J Moll Cell Cardiol* 2002;34:1241–1247.
30. Iaccarino G, Ciccarelli M, Sorriento D, Cicolletta E, Cerullo V, Iovino GL, et al. Akt participates to endothelial dysfunction in hypertension. *Circulation* 2004;109:2587–2593. [PubMed: 15136501]
31. Claudio PP, Fratta L, Farina F, Howard CM, Stassi G, Numata S, et al. Adenoviral RB2/p130 gene transfer inhibits smooth muscle cell proliferation and prevents restenosis after angioplasty. *Circ Res* 1999;85:1032–1039. [PubMed: 10571534]
32. Cittadini A, Stromer H, Katz SE, Clark R, Moses AC, Morgan JP, et al. Differential cardiac effects of GH and IGF-1 in the rat: a combined *in vivo* and *in vitro* evaluation. *Circulation* 1996;93:800–809. [PubMed: 8641010]
33. Kihara Y, Grossman W, Morgan JP. Direct measurement of changes in intracellular calcium transients during hypoxia, ischemia and reperfusion of the intact mammalian heart. *Circ Res* 1989;65:1029–1044. [PubMed: 2791218]
34. Brooks WW, Healey NA, Sen S, Conrad CH, Bing OH. Oxygen cost of stress development in hypertrophied and failing hearts from the spontaneously hypertensive rat. *Hypertension* 1993;21:56–64. [PubMed: 8418024]
35. Nelson GS, Berger RD, Fetis B, Talbot M, Spinelli JC, Hare JM, et al. Left ventricular or biventricular pacing improves cardiac function at diminished energy cost in patients with dilated cardiomyopathy and left bundle-branch block. *Circulation* 2000;102:3053–3059. [PubMed: 11120694]
36. Callies F, Stromer H, Schwinger RH, Bolck B, Hu K, Frantz S, et al. Administration of testosterone is associated with a reduced susceptibility to myocardial ischemia. *Endocrinology* 2003;144:4478–4483. [PubMed: 12960063]
37. Chomczynski P, Sacchi N. Single step method of RNA isolation by acidic guanidinium thiocyanate–phenol–chloroform extraction. *Anal Biochem* 1987;162:156–159. [PubMed: 2440339]

38. Temsah RM, Dyck C, Neticadan T, Chapman D, Elimban V, Dhalla NS. Effect of  $\beta$ -adrenoreceptor blockers on sarcoplasmic reticular function and gene expression in the ischemic reperfused heart. *J Pharmacol Exp Ther* 2000;293:15–23. [PubMed: 10734148]
39. Iaccarino G, Barbato E, Cipolletta E, Esposito A, Fiorillo A, Koch WJ, et al. Cardiac  $\beta$ ARK1 upregulation induced by chronic salt deprivation in rats. *Hypertension* 2001;38:255–260. [PubMed: 11509486]



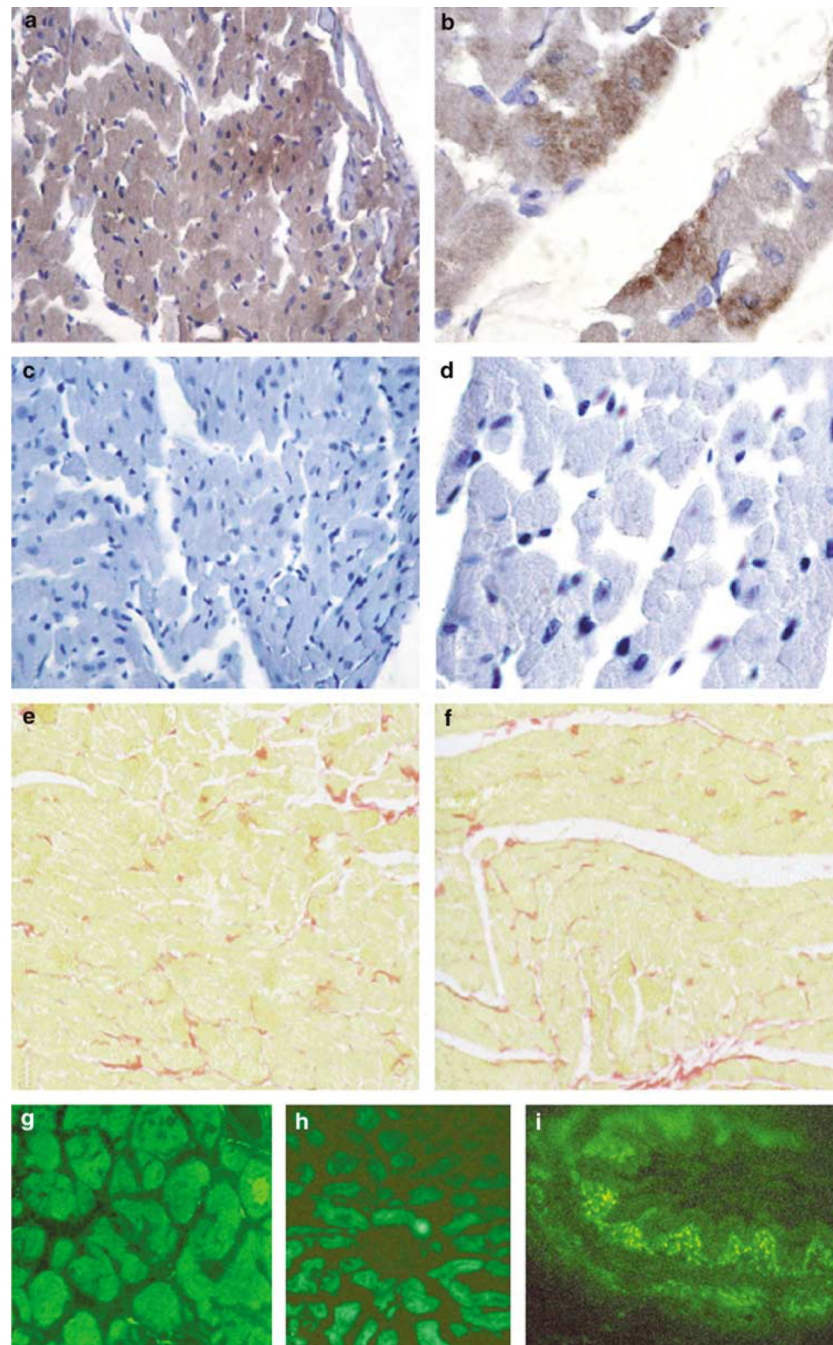


**Figure 1.** Cardiac gene expression of Ad.Akt enhanced with an anti-HA antibody, in panel a: showed at  $\times 300$  magnification and in panel b at  $\times 900$ . Control sections, obtained by omitting primary antibody, are depicted in panel c (low magnification) and in panel d (high magnification). Panels e and f show cardiac collagen content in control and Ad.Akt group, respectively. No differences are found among the three study groups (Ad.HA not showed). Panels g (heart), h (liver), i (kidney) show cardiac and extracardiac expression after cardiac injection of a viral construct carrying GFP.

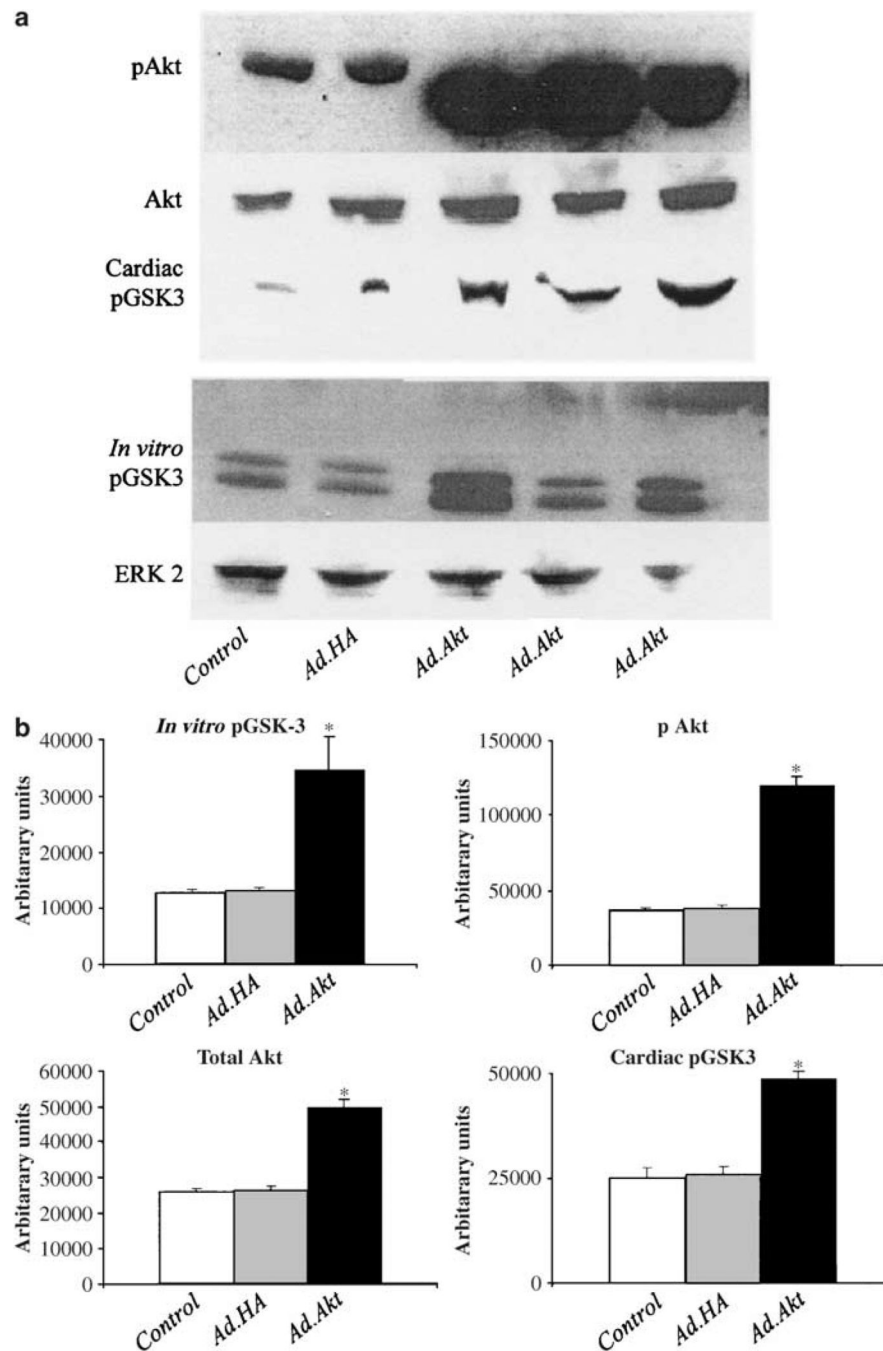


**Figure 2.** Akt activity. Panel a: representative Western blotting showing cardiac pGSK-3, phosphorylated Akt (pAkt), total Akt, *in vitro* Akt kinase assay (*in vitro* pGSK-3), and ERK2 amount in the three study groups. Ad.Akt immunoblots are presented in triplicate, to show the interindividual variability. The diagrams in panel b depict densitometrical data, expressed in arbitrary units. Values are mean±s.e.m. \* $P < 0.01$  versus control and Ad.HA.

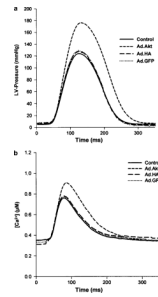


**Figure 3.**

Intracellular  $\text{Ca}^{2+}$  transients (panel b) and LV pressure tracings (panel a) at baseline perfusate calcium (2 mmol/l) in aequorin-loaded control (solid lines), Akt- (dashed lines) Ad.GFP-(dotted lines) and Ad.HA-infected (long-dashed lines) whole hearts ( $n=10$ , except Ad.GFP,  $n=5$ ). See Materials and methods for experimental conditions. The  $x$ -axis indicates time after pacing stimulus;  $\text{Ca}^{2+}$  transients, 30–60 wave-averaged cycles of nonfiltered light signals, were converted to  $\text{Ca}^{2+}$  concentration values by fractional luminescence (see text). For statistical differences, see Tables 1 and 2.

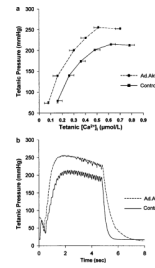


**Figure 4.**

Steady-state pressure– $[Ca^{2+}]_i$  relations in Akt-infected perfused (dashed lines;  $n=10$ ) whole hearts preparations and controls (solid lines;  $n=10$ ). In panel a, peak tetanic pressure is plotted against  $[Ca^{2+}]_i$  during tetanic plateau phase of light signal. In panel b, representative tracing of tetanic pressure in Ad.Akt (dashed lines) and controls (solid lines) whole hearts. Tetanus was triggered by 4 s of electrical stimulation at 15 Hz, with a pulse width of 50 ms. Calcium in the perfusate was 6.0 mM. Values of maximal calcium activated tetanic pressure were (mean $\pm$ s.e.m.) 214 $\pm$ 3 and 208 $\pm$ 2 versus 255 $\pm$ 2 mmHg in control and Ad.HA- versus Ad.Akt-infected perfused hearts, respectively ( $P<0.01$ );  $EC_{50}$  was 0.52 $\pm$ 0.03 and 0.53 $\pm$ 0.03 versus 0.47 $\pm$ 0.02  $\mu\text{mol/l}$  in control and Ad.HA-versus Ad.Akt-infected perfused hearts, respectively.

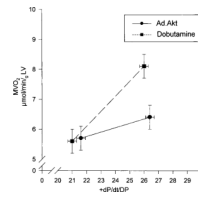


**Figure 5.**

Comparison of mechanoenergetic responses to Akt myocardial infection versus dobutamine application to the perfu-sate. Absolute values are shown for  $dP/dt_{max}$ /developed pressure (abscissa) and  $MVO_2$  (ordinate). Both sets of studies had similar contractile indexes baseline and increase because of intervention. However, dobutamine raised  $MVO_2$  2.6-fold compared with Akt infection ( $P<0.01$ ).

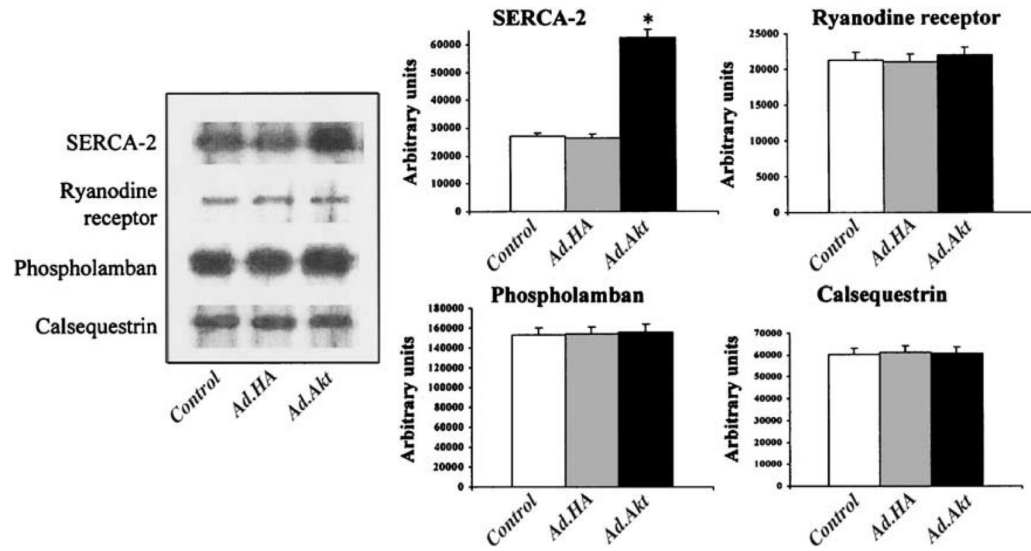


**Figure 6.** Graph and representative Western blots showing ryanodine receptor, SERCA-2, phospholamban, and calsequestrin protein levels in LV tissue in the three study groups. Values are mean±s.e.m. \* $P<0.01$  versus control and Ad.HA.



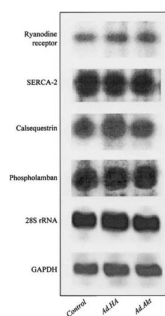


**Figure 7.** Northern blots from left ventricle RNAs hybridized with probes corresponding to ryanodine receptor, SERCA-2, phospholamban, and calsequestrin. 28S rRNA was used as loading control. The intensity of each signal was normalized by GAPDH signal intensity. No significant differences were found.

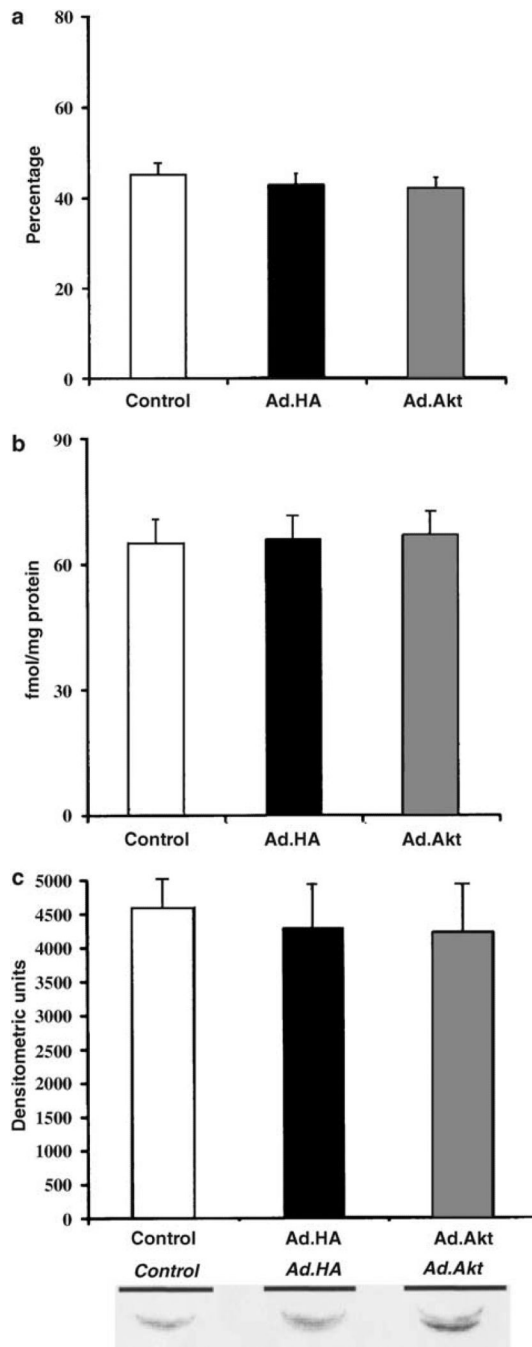


**Figure 8.** LV  $\beta$ -adrenergic receptor high-affinity binding (panel a), density (panel b), and kinase-1 protein content (panel c) showing no significant differences among the three study groups.

Table 1

Isolated whole heart mechanical data

	$P_{\text{systemic}}$ (mmHg)	$P_{\text{diastolic}}$ (mmHg)	$P_{\text{developed}}$ (mmHg)	$+dP/dt$ (mmHg/S)	$-dP/dt$ (mmHg/S)	TP (ms)	T90 (ms)	Tau (ms)	CPP (mmHg)
Controls	121±4	5±0.7	116±4	2590±107	1430±58	80±3	112±3	41±2	75±2
Ad.HA	119±3	5±1	114±5	2500±150	1400±70	78±4	109±4	40±3	75±3
Ad.GFP	118±4	5±1.2	116±6	2530±170	1390±85	80±5	110±5	40±3	74±4
Ad.Akt	171±3*	6±0.6	165±3*	3970±111*	2050±60*	86±3*	130±3*	46±2	74±2

Values are mean±s.e.m.;  $n = 10$ ;  $P$  = pressure; TP = time to peak pressure; T90 = time to 90% relaxation; Tau = time constant of exponential left ventricular pressure decay; CPP = coronary perfusion pressure.

\*  $P < 0.05$  versus controls.

Table 2

Measurements of intracellular  $\text{Ca}^{2+}$  handling

	$\text{Ca}_{\text{systole}}$ ( $\mu\text{mol/l}$ )	$\text{Ca}_{\text{diastole}}$ ( $\mu\text{mol/l}$ )	$\text{TP}_{\text{Ca}}$ (ms)	$\text{T50}_{\text{Ca}}$ (ms)	$\text{TP}_{\text{Ca}^+ \text{T50}_{\text{Ca}}}$ (ms)	$\text{Tau}_{\text{Ca}}$ (ms)	$\text{EC}_{50}$ ( $\mu\text{mol/l}$ )	$\text{MCAP}$ (mmHg)
Controls	$0.76 \pm 0.03$	$0.35 \pm 0.001$	$46 \pm 2$	$41 \pm 3$	$88 \pm 5$	$38 \pm 5$	$0.52 \pm 0.03$	$214 \pm 3$
Ad.HA	$0.77 \pm 0.03$	$0.35 \pm 0.002$	$46 \pm 3$	$42 \pm 2$	$89 \pm 4$	$38 \pm 4$	$0.53 \pm 0.03$	$208 \pm 2$
Ad.GFP	$0.77 \pm 0.05$	$0.35 \pm 0.003$	$47 \pm 3$	$41 \pm 4$	$87 \pm 6$	$38 \pm 7$	$0.52 \pm 0.04$	$210 \pm 5$
Ad.Akt	$0.91 \pm 0.03^*$	$0.35 \pm 0.001$	$50 \pm 3$	$44 \pm 4$	$98 \pm 5$	$37 \pm 2$	$0.47 \pm 0.02$	$255 \pm 4^*$

Values are mean  $\pm$  s.e.m.;  $n = 10$ ; Ca = calcium; TP = time to peak light; T50 = time from peak light to 50% of light decay; Tau = time constant of exponential light decay; EC50 = EC50 of the calcium concentration–response relationship; MCAP = maximal calcium activated tetanic pressure.

\*  $P < 0.05$  versus controls and Ad.HA.